

# REAL COMPTON SCATTERING FROM THE PROTON

Alan M. NATHAN

*University of Illinois at Urbana-Champaign, 1110 W. Green Street,  
Urbana, IL 61801, USA*

*E-mail: a-nathan@uiuc.edu*

Real Compton Scattering on the proton in the hard scattering regime is investigated. Recent theoretical developments are reviewed. Plans for new experimental studies at Jefferson Lab are presented.

## 1 Introduction

Real Compton Scattering (RCS) in the hard scattering limit is a powerful probe of the short-distance structure of the nucleon. It is a natural complement to other hard exclusive reactions that are currently being pursued at Jefferson Laboratory (JLab) and elsewhere, such as high  $Q^2$  elastic form factors, hard pion electroproduction and photoproduction, and Virtual Compton Scattering (VCS), and Deeply Virtual Compton Scattering (DVCS). The common feature of these reactions is a hard energy scale, leading to the factorization of the scattering amplitude into a part involving a hard perturbative scattering amplitude, which describes the coupling of the external particles to the active quarks, and the overlap of soft nonperturbative wave functions, which describes the coupling of the active quarks to the proton. For RCS, the hard scale is achieved when the Mandelstam variables  $s$ ,  $-t$ , and  $-u$  are all large, or equivalently when  $p_\perp$  is large, on the hadronic scale.

There has been considerable theoretical effort in recent years in calculating RCS cross sections and polarization observables in the hard scattering limit, and one goal of this contribution is to review this activity (Section 2). Despite this renewed theoretical interest in RCS, the only Compton scattering data available in this kinematic regime are the 20-year old Cornell data,<sup>1</sup> which are sparse and of limited statistical precision in the theoretically interesting range of high  $p_\perp$ . In order to provide the high quality data necessary to discriminate among reaction mechanisms and gain new insight into the structure of the proton, a new experiment is planned at JLab (E97-108/E99-114) to measure RCS cross sections over a broad range of  $s$  and  $t$  and to have an initial look at polarization observables. A second goal of this contribution is to present an overview of the new experiment in the context of the theoretical work (Section 3). A summary is presented in Section 4.

## 2 Theoretical Overview

Various theoretical approaches have been applied to RCS in the hard scattering regime, and these can be distinguished by the number of active quarks participating in the hard scattering subprocess, or equivalently, by the mechanism for sharing the transferred momentum among the constituents. Two extreme pictures have emerged. In the perturbative QCD (pQCD) approach,<sup>2,3,4</sup> there are three active quarks which share  $t$  by the exchange of two hard gluons (see Fig. 1a). In the soft overlap approach,<sup>5,6</sup> the handbag diagram dominates (see Fig. 1b) in which there is one active quark and  $t$  is shared by the overlap of the high momentum components of the soft wave function. In any given kinematic regime, both mechanisms will contribute, in principle, to the cross section. It is generally believed that at sufficiently high energies, the pQCD mechanism dominates. However, the question of how high is “sufficiently high” is still an open question to be answered by more precise experiments, and it is not known with any certainty what is the dominant mechanism in the kinematic regime appropriate to JLab ( $p_{\perp} \sim 1 - 2$  GeV).

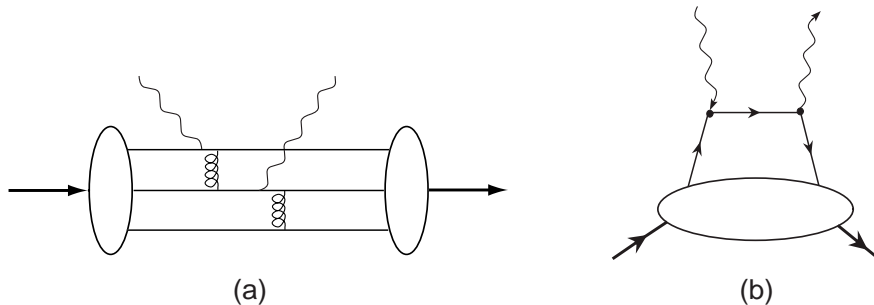


Figure 1: Different hard scattering mechanisms for RCS. In the pQCD mechanism (a), the momentum is shared among the quarks by hard gluon exchange. In the handbag mechanism (b), the scattering is from a single quark and the momentum is shared by the overlap of the high momentum components of the soft wave function.

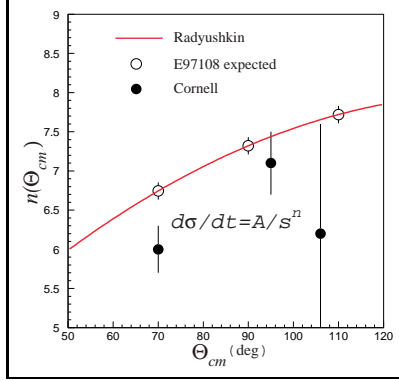


Figure 2: Scaling of RCS cross section at fixed  $\theta_{cm}$ . The closed points are the Cornell data. The open points represent the projected precision from the JLab experiment. The curve is the prediction of Radyushkin, assuming dominance of the handbag diagram. For the pQCD mechanism,  $n=6$  independent of  $\theta_{cm}$ .

Cornell data.<sup>2,4</sup> This has led to the suggestion<sup>5,6</sup> that the dominant mechanism at experimentally accessible energies is the soft overlap mechanism, which I describe next.

In the soft overlap approach to hard exclusive reactions in general and to RCS in particular, the handbag diagram dominates. The hard physics is contained in the scattering from a single active quark, whereas the soft physics is contained in the wave function describing how the active quark couples to the proton. This coupling is described in terms of nonforward parton densities (ND)<sup>8,9</sup> which are superstructure of the nucleon from which are derived the normal parton densities, elastic form factors, and other quantities that have yet to be measured, including new form factors accessible through Compton scattering. Therefore the ND provide links among diverse physical processes, including both inclusive and exclusive reactions. For example, the dominant ND in RCS is  $\mathcal{F}^a(x, t)$ , which is related to both the Dirac form factor  $F_1$  and the RCS vector form factor  $R_V$  through the expressions

$$F_1(t) = \sum_a e_a \int_0^1 \mathcal{F}^a(x; t) dx \quad R_V(t) = \sum_a e_a^2 \int_0^1 \mathcal{F}^a(x; t) \frac{dx}{x}, \quad (2)$$

whereas the  $t = 0$  limit of  $\mathcal{F}^a(x, t)$  is the parton distribution function  $q^a(x)$ . Additional links are shown in Table 1. Despite the similarity between the  $(e, e)$

I next examine the two reaction mechanisms in somewhat more detail. In the pQCD approach, the exchange of two hard gluons leads naturally to the constituent counting rule and scaling<sup>7</sup>

$$\frac{d\sigma}{dt} = \frac{f(\theta_{cm})}{s^n}, \quad (1)$$

where  $n=6$  for RCS. The valence Fock state dominates, since higher Fock states require additional gluon exchanges and are therefore suppressed by additional factors of  $1/s$ . The soft physics enters through the valence quark distribution amplitude (DA)  $\phi(x_1, x_2, x_3)$ . Experimentally, the Cornell data support scaling with  $n \approx 6$  (Fig. 2), albeit with modest statistical precision. Nevertheless, it has been shown that the cross sections calculated using the asymptotic DA badly underpredict the

and RCS form factors, an important distinction is the weighting by the quark charge, which is linear for  $(e, e)$  and quadratic for RCS, reflecting the one- and two-photon nature of the interaction, respectively. Thus RCS is sensitive to the flavor structure of the proton in a different way than electro-weak scattering, thereby potentially providing another tool, along with parity-violating electron scattering, for decomposing the flavor structure. In particular, RCS has a greater sensitivity to sea quarks than does  $(e, e)$ .

Table 1: Nonforward parton densities (ND) and their associated electroweak scattering (EWS) and RCS form factors, where  $a$  labels the quark flavor. The last column shows the relationship with the parton distribution functions.

ND	EWS Form Factor	RCS Form Factor	$t = 0$ limit
$\mathcal{F}^a(x; t)$	$F_1(t)$	$R_V(t)$	$q^a(x)$
$\mathcal{K}^a(x; t)$	$F_2(t)$	$R_T(t)$	$2J^a(x)/x - q^a(x)$
$\mathcal{G}^a(x; t)$	$G_A(t)$	$R_A(t)$	$\Delta q^a(x)$

The relationship between the RCS cross section and the form factors has been worked out with several simplifying approximations, including the neglect of terms such as  $R_T$  which involve hadron helicity flip. This leads to the factorization of the RCS cross sections into a simple product of the Klein-Nishina (KN) cross section describing the hard scattering from a single quark and a sum of form factors depending only on  $t$ <sup>5,6</sup>:

$$\frac{d\sigma}{d\sigma_{\text{KN}}} = f_V R_V^2(t) + (1 - f_V) R_A^2(t) \quad f_V = \frac{(\tilde{s} - \tilde{u})^2}{2(\tilde{s}^2 + \tilde{u}^2)}, \quad (3)$$

where  $\tilde{s} = s - m^2$  and  $\tilde{u} = u - m^2$ . The vector and axial vector form factors  $R_V$  and  $R_A$ , respectively, have a simple physical interpretation. The combination  $|R_V(t) + R_A(t)|^2$  is the probability that a photon can scatter elastically from the proton by transferring  $t$  to a single active quark whose helicity is oriented in the direction of the proton helicity. Similarly  $|R_V(t) - R_A(t)|^2$  is the probability that the active quark has helicity opposite to that of the proton. In order to measure  $R_V$  and  $R_A$ , it is necessary to measure the RCS cross section at fixed  $t$  with a variable  $f_V$  in order to achieve a “Rosenbluth-like” separation. However, for the kinematics of interest, where  $s$ ,  $-t$ , and  $-u$  are all large,  $f_V$  is always close to 1. Consequently the unpolarized cross sections are largely insensitive to  $R_A$ . This leads to the very nice feature that the left-hand-side of Eq. 3 is nearly  $s$ -independent at fixed  $t$ . This is shown in Fig. 3, where one sees that the pQCD mechanism predicts a very different behavior, thereby

allowing a very powerful test of the reaction mechanism as well as a precise measurement of  $R_V$ .

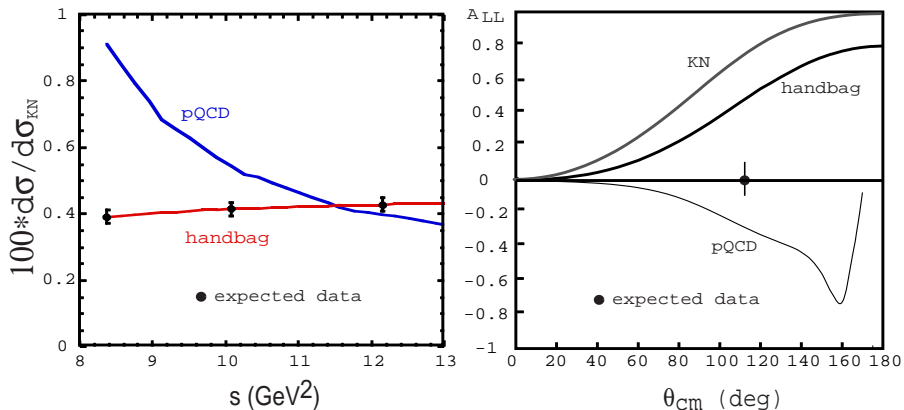


Figure 3: (Left) The ratio  $d\sigma/d\sigma_{KN}$ , scaled by a factor of 100, as a function of  $s$  at  $-t = 5$  GeV<sup>2</sup>. This ratio is nearly independent of  $s$  in the handbag but not in the pQCD model. (Right) The longitudinal spin transfer parameter at 4 GeV. The handbag model essentially follows the Klein-Nishina (KN) result for a structureless Dirac particle. For both plots the points show the precision of the data expected from JLab E99-114.

Simple models for the ND's have been proposed, leading to predictions for the RCS form factors and cross sections.<sup>5,6</sup> An interesting feature of these form factors is that they decrease approximately as  $1/t^2$  in the few-10 GeV<sup>2</sup> range, leading to  $n \approx 6$  scaling factor, in agreement with the asymptotic law (Eq. 1) but for very different reasons. However, nontrivial violations of  $n = 6$  scaling are predicted in the form of an angle-dependent scaling factor  $n(\theta_{CM})$ , which seems to agree with the limited Cornell data (Fig. 2). Another interesting feature is that at sufficiently high  $-t$ , the form factors fall as  $1/t^4$ , leading to  $n \approx 10$ . Thus the handbag contribution to RCS will be asymptotically subdominant to the pQCD contribution, even though the former may dominate at experimentally accessible energies.

A measurement of polarization observables provides further tests of the reaction mechanism as well as access to additional form factors. The longitudinal polarization transfer observable  $A_{LL}$  is defined by

$$A_{LL} \frac{d\sigma}{dt} \equiv \frac{d\sigma(\uparrow\uparrow)}{dt} - \frac{d\sigma(\uparrow\downarrow)}{dt} \quad (4)$$

where the first arrow refers to the incident photon helicity and the second to

the recoil proton helicity. In the handbag mechanism, this is related to the form factors by the expression<sup>6</sup>

$$A_{LL} \frac{d\sigma}{d\sigma_{\text{KN}}} = A_{LL}^{\text{KN}} R_V(t) R_A(t), \quad (5)$$

where  $A_{LL}^{\text{KN}}$  is the result for a structureless Dirac particle. This is plotted in Fig. 3, where one sees that the handbag calculation essentially follows the KN result, whereas the pQCD prediction looks very different, thereby providing another stringent test of the reaction mechanism in addition to a measurement of the axial form factor  $R_A$ . One can similarly define the transverse polarization transfer observable  $A_{LT}$ , which arises as an interference between proton helicity flip and non-flip amplitudes. In the strict pQCD limit, it must vanish since hadron helicity is conserved. Thus far this observable has not been calculated with either the pQCD or handbag mechanisms. However, one can anticipate that in the handbag mechanism it will be proportional to  $R_T$ , the RCS form factor that is closely related both to the Pauli elastic form factor  $F_2$  and to the quark total angular momentum (see Table 1), both of which are topics of high current interest. The induced polarization  $P_N$  is the component of recoil polarization normal to the scattering plane and involves the imaginary part of the interference between helicity flip and nonflip amplitudes. In the handbag mechanism, it is suppressed since all amplitudes are strictly real in this model.<sup>6</sup> In the strict pQCD limit, it vanishes due to hadron helicity conservation. No calculation has yet been done for this quantity.

### 3 A New Experiment: JLab E99-114

Experiment E97-108 (recently upgraded to E99-114) at JLab plans to measure differential cross sections for Compton scattering from the proton at incident photon energies between 3 and 6 GeV ( $s=6-12 \text{ GeV}^2$ ) and over a wide range of CM scattering angles ( $-t=2-7 \text{ GeV}^2$ ). The goal is to achieve a statistical precision of order 5%, with systematic errors less than 6%. In addition a measurement of the components of the proton recoil polarization at  $s = 8$ ,  $-t = 4 \text{ GeV}^2$  is planned, using a polarized photon beam. Both sets of measurements utilize the technique shown schematically in Fig. 4.

A high duty factor electron beam with current  $\geq 10 \text{ } \mu\text{A}$  is incident on a 6% copper radiator located just upstream of the scattering target. The mixed beam of electrons and bremsstrahlung photons is incident on a 15-cm LH<sub>2</sub> target. For incident photons near the bremsstrahlung endpoint, the recoil proton and scattered photon are detected with high angular precision in a magnetic spectrometer and photon spectrometer, respectively.

The magnetic spectrometer is one of the High Resolution Spectrometers that are part of the standard Hall A equipment, along with the cryogenic hydrogen target and bremsstrahlung radiator. The photon spectrometer is a new piece of equipment which is being constructed for this experiment. For the polarization measurements, a longitudinally polarized electron beam is used and the polarization is nearly completely transferred to the bremsstrahlung photon. The components of the polarization of the recoil proton are measured in the focal plane polarimeter (FPP) which

is also part of the standard Hall A equipment. One essential feature of the experimental technique is the use of the kinematic correlation between the scattered photon and recoil proton in the RCS reaction to reduce the background of  $\pi^0$  decay photons from the  $p(\gamma, \pi^0 p)$  reaction, thereby placing stringent demands on the combined angular resolution of two-spectrometer system. A second essential feature is the mixed electron-photon beam, which is required in order to achieve the desired photon luminosity. On the one hand, this introduces the necessity to identify and reject electrons from  $ep$  elastic scattering, while on the other hand it provides a convenient tool for an *in situ* calibration of the photon spectrometer and normalization of cross sections.

The principal new piece of equipment for this experiment is the photon spectrometer, which is currently under construction. The principal component is a large-area segmented Pb-glass calorimeter with excellent position resolution and modest energy resolution. In order to reduce the potential background of electrons from  $ep$  elastic scattering, which are kinematically indistinguishable from RCS photons, several techniques will be used. First, the number of  $ep$  elastic electrons will be considerably reduced by avoiding the region very close to the bremsstrahlung endpoint, where the  $e/\gamma$  ratio in the beam is very large. Next, electrons will be identified in a plexiglass Čerenkov veto detector that is segmented to allow for a veto that is spatially correlated with an event in the calorimeter. Finally, a magnet will be used to deflect the  $ep$  elastic electrons by a sufficient amount on the front face of the calorimeter to allow identification by the altered kinematic correlation with the recoil proton relative to undeflected RCS photons. The mixed  $\gamma - e$  beam is advantageous in that the  $ep$  elastic electrons can be used to calibrate the photon spectrometer and normalize the RCS cross sections. For this purpose, several planes of

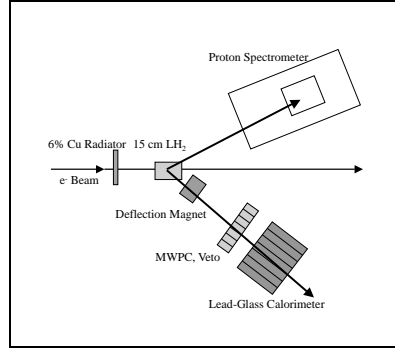


Figure 4: Schematic of the planned JLab experiment.

MWPC just in front of the calorimeter will be used in a separate *in situ ep* elastic scattering experiment to calibrate the position of each element of the calorimeter and veto detector, measure the position resolution, and measure the veto efficiency.

The technique outlined here is conceptually similar to that used in the Cornell experiment. However, the combined effects of a high duty factor electron beam, a state-of-the-art magnetic spectrometer, the ability to calibrate *in situ* with *ep* elastic scattering, and high segmentation in the photon detector should allow significantly better measurements in the range of  $s$  and  $t$  already covered by Cornell, as well as significant extensions beyond that. The equipment would also be suitable for measurements at higher energies, should those energies become available at JLab in the future.

## 4 Summary

In this contribution, I have summarized our present theoretical understanding of the RCS process in the hard scattering regime. In addition, I have presented the conceptual design of a new experiment that should extend the RCS data base in the very near future.

## Acknowledgments

It is a pleasure to acknowledge stimulating discussion with M. Diehl, P. Kroll, M. Vanderhaeghen, and especially A. Radyushkin. I also thank my E99-114 colleagues C. Hyde-Wright, B. Wojtsekhowski, and F. Sabatie. This work was supported in part by the USNSF under Grant No. 94-20787.

## References

1. M.A. Shupe *et al.*, Phys. Rev. **D19** (1979) 1929.
2. A. S. Kronfeld and B. Nizic, Phys. Rev. **D44** (1991) 3445.
3. G. R. Farrar and H. Zhang, Phys. Rev. Lett. **65** (1990) 1721;  
Glennys R. Farrar and H. Zhang, Phys. Rev. **D41** (1990) 3348; and  
E. Maina and G. R. Farrar, Phys. Lett. **B206** (1988) 120.
4. M. Vanderhaeghen, *et al.*, Nucl. Phys. **A622** (1997) 144c.
5. A. Radyushkin, Phys. Rev. D **58** (1998) 114008.
6. M. Diehl, Th. Feldman, R. Jakob, and P. Kroll, hep-ph/9811253, hep-ph/9903268. P. Kroll, these proceedings.
7. S.J. Brodsky and G. Farrar, Phys. Rev. Lett. **31** (1973) 1953.
8. X. Ji, Phys. Rev. Lett. **78** (1997) 610; Phys. Rev. D **55** (1997) 7114.
9. A. Radyushkin, Phys. Rev. D **56** (1997) 5524.